analytical chemistry

Article

pubs.acs.org/ac

Protein Electrocatalysis for Direct Sensing of Circulating MicroRNAs

Mahmoud Labib, Nasrin Khan, and Maxim V. Berezovski*

Department of Chemistry, University of Ottawa, 10 Marie Curie, Ottawa, Ontario K1N 6N5, Canada

Supporting Information

ABSTRACT: MicroRNAs (miRNAs) are potentially useful biomarkers for diagnosis, classification, and prognosis of many diseases, including cancer. Herein, we developed a protein-facilitated electrocatalytic quadroprobe sensor ($Sens^{PEQ}$) for detection of miRNA signature of chronic lymphocytic leukemia (CLL) in human serum. The developed signal-ON sensor provides a compatible combination of two DNA adaptor strands modified with four methylene blue molecules and electrocatalysis using glucose oxidase in order to enhance the overall signal gain. This enhanced sensitivity provided the response necessary to detect the low-abundant serum miRNAs without preamplification. The developed $Sens^{PEQ}$ is exquisitely sensitive to subtle π-stack perturbations and capable of distinguishing single base mismatches in the target miRNA. Furthermore, the developed sensor was employed for profiling of three endogenous miRNAs characteristic to CLL, including hsa-miR-16-5p, hsa-miR-21-5p, and hsa-miR-150-5p in normal healthy serum, chronic lymphocytic leukemia Rai stage 1 (CLL-1), and stage 3 (CLL-3) sera, using a non-human cel-miR-39-3p as an internal standard. The sensor results were verified by conventional SYBR green-based quantitative reverse-transcription polymerase chain reaction (RT-qPCR) analysis.

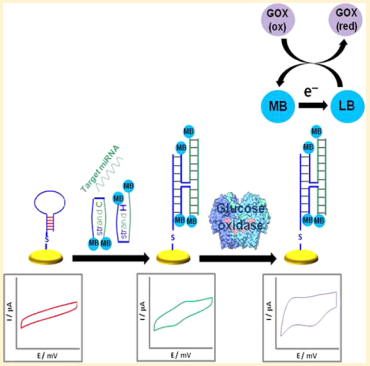

MicroRNAs (miRNAs) represent a major class of noncoding RNAs that regulate the expression of target genes at the post-transcriptional level by translational repression or degradation of mRNAs (mRNAs).[1] Mature miRNAs are ~22 nucleotides long and they play pivotal roles in a wide range of biological processes from cell proliferation and death to cancer progression.[2] Deregulation of specific subsets of miRNAs, known as "miRNA fingerprints", has been demonstrated to cause several human malignancies and disorders, including cancer,[3] cardiovascular diseases,[4] neurological disorders,[5] and diabetes.[6] In addition, altered expression levels of miRNAs, including up-regulation and down-regulation, have been correlated with cancer type and stage. Hence, they are vital biomarkers for cancer diagnosis, prognosis, and therapy.[7] Furthermore, being shorter than most RNAs, miRNAs are less vulnerable to degradation by ribonucleases. In addition, miRNAs usually circulate in blood within exosomes or in a complex with an RNA-binding protein, nucleophosmin 1.[8] Therefore, they are extremely stable and can be detected directly in blood and other body fluids, thus making noninvasive collection of samples possible.[9] Detection of miRNAs in diagnostics is based on the different expression profiles of miRNAs in patients compared to healthy subjects. However, their small size, low abundance, and sequence homology make miRNAs profiling a challenging task.

Standard methods for miRNA detection include Northern blotting, which has low sensitivity and requires large samples. In addition, it is laborious and time-consuming, which makes it difficult to implement for routine miRNA analysis.[10] Despite the high sensitivity of the in situ hybridization technique, it is relatively slow and time-consuming.[11] On the other hand, oligonucleotide microarrays have the advantage of high throughput; however, this technology is limited by the problems of low sensitivity and undesired cross-hybridization.[12] Alternative methods include quantitative reverse-transcription PCR (RT-qPCR)[13] and deep sequencing.[14] However, these methods are laborious and involve several amplification steps. Also, they require the use of well-equipped laboratories and highly trained personnel and thus they are not suitable for point-of-care (POC) settings.[15,16] Several modern techniques have been developed for miRNA analysis, including surface plasmon resonance imaging (SPRI),[17] surface-enhanced Raman spectroscopy (SERS),[18] bioluminescence-based techniques,[19] and fluorescence correlation spectroscopy.[20] However, these methods require costly equipment and sophisticated readout systems and they are not feasible for routine determination of miRNAs.[21] Compared to the aforementioned methods, electrochemical nucleic acid sensors hold great promise to serve as platforms for miRNA expression profiling due to their simplicity, selectivity, high sensitivity, cost effectiveness, and ease of miniaturization.[22−30] The stringency of electrochemically controlled nucleic acid detection allows single base mismatch specificity even in clinical samples.[31]

Several electrochemical sensors for miRNA detection have been developed based on the formation of DNA four-component hybridization product,[32] or signal amplification using enzymes,[33] proteins,[31] inorganic nanomaterials,[34] and metallic compounds.[35] In addition, oxidation of the guanine bases in the captured strand was utilized to detect miRNA.[36] Also, miRNA was successfully detected based on the change on

Received: November 19, 2014
Accepted: December 14, 2014
Published: December 14, 2014

DOI: 10.1021/ac504331c
Anal. Chem. 2015, 87, 1395−1403

the interfacial resistance after hybridization.[37] Moreover, the Fe−Ru redox pair was used as an electrocatalytic reporter to detect miRNAs with high sensitivity.[38] Furthermore, a series of electrochemical sensors for miRNA analysis have been developed by labeling the target miRNA with OsO_2,[39] RuO_2,[40] and $Os(dmpy)_2(IN)Cl^+$ nanoparticles.[35] However, these methods require prelabeling of the target miRNA prior to detection which might complicate the assay, particularly in clinical analysis.[41] In addition, the majority of the label-free sensors are based on signal modulation, where the capture of the target strand is usually accompanied by a change in the existing electrical signal. For this reason, these sensors are relatively incapable of direct detection of nucleic acids in biological fluids since the sensors can be easily fouled with the other biological components in the sample, leading to a change in the current signal. In this work, we developed a protein-facilitated electrocatalytic quadroprobe sensor ($Sens^{PEQ}$) for detection of miRNA signature in chronic lymphocytic leukemia (CLL). Despite CLL being an incurable disorder, early stage detection and treatment can control diseases progression, whereas late stage patients often do not respond to various treatments.[42] In spite of the heterogeneous pathology of the disease, currently CLL patients are treated with a few standardized treatments, on the basis of limited clinical parameters such as Rai or Binet staging, which classify CLL patients on the basis of the spreading of the disease and its cytogenetic characterization.[43,44] In need for more informative diagnostic markers with better clinical significance for CLL, Moussay et al. explored the possibility of using the changes of extracellular miRNA spectra in a CLL plasma sample. They showed that specific plasma miRNA signatures are associated with CLL and can be used as new and informative biomarkers for CLL diagnosis.[45] The involvement of miRNAs in CLL pathogenesis was also suggested by Klein et al.[46] In addition, many other studies have reported the use of miRNA expression profiling in CLL.[47−50] To that end, the developed $Sens^{PEQ}$ was employed for profiling of three CLL specific circulating miRNAs, including miR-16-5p, miR-21-5p, and miR-150-5p.[45] Several optimization studies were performed to enhance the sensitivity of the assay, including the number and position of the methylene blue (MB) molecules, electrode material, and electrocatalyst type. Finally, the $Sens^{PEQ}$ was successfully employed for direct detection and profiling of hsa-miR-16-5p, hsa-miR-21-5p, and hsa-miR-150-5p in human healthy serum and CLL serum, Rai stage I and Rai stage III, in the presence of cel-miR-39 as an internal standard. Finally, the sensor results were verified by conventional SYBR green-based quantitative reverse-transcription polymerase chain reaction (RT-qPCR) analysis.

EXPERIMENTAL SECTION

Sensor Preparation. Prior to experiments, the screen-printed gold nanoparticles modified carbon nanofibers electrode (GNPs-CNFs, *L* 33 × *W* 10 × *H* 0.5, Dropsens, Spain) was washed thoroughly with deionized nuclease-free water then dried with N_2. This was followed by reduction of the universal interfacial probe (UIP), which contains a phosphate group at the 5′ position and a 6-hydroxyhexyl disulfide group at the 3′ position. Briefly, 2 μL of 100 μM UIP was mixed with 4 μL of 10 mM tris-(2-carboxyethyl)phosphine (TCEP, Sigma-Aldrich, U.S.) and the solution was incubated for 1 h at room temperature. The role of TCEP is to reduce the disulfide bond of the UIP because it can selectively reduce even the most stable water-soluble alkyl disulfides over a wide pH range.[51] Afterward, the electrode was incubated with 1 μM reduced UIP in the incubation buffer, 50 mM phosphate buffer (pH 7) containing 150 mM NaCl, and 10 mM $MgCl_2$, in a humidity chamber overnight. Finally, the electrode was incubated with 0.1 mM 2-mercaptohexanol for 30 min to reduce the background oxygen contributions and nonspecific interactions between the probe and the gold surface and allow the probe to adopt an upright position.[52] All miRNAs used in the experiments were purchased from Integrated DNA Technologies, U.S. whereas, the methylene blue labeled adaptor strands were purchased from Biosearch Technologies, U.S. Sequences of the nucleic acids utilized in the experiments are provided in Table S1 (Supporting Information).

Electrochemical Measurements. Cyclic voltammetry (CV) was performed with an electrochemical analyzer (CH Instruments 660D, TX, U.S.) connected to a personal computer. All measurements were carried out at room temperature in an enclosed and grounded Faraday cage. A conventional three-electrode configuration printed on a ceramic substrate was used including a GNPs-CNFs electrode as the working electrode, a carbon counter electrode, and a silver pseudoreference electrode. A three-electric contacts edge connector (Dropsens, Spain) was used to connect the screen-printed electrode with the potentiostat. The open-circuit or rest-potential of the system was measured prior to all electrochemical experiments to prevent sudden potential-related changes in the self-assembled monolayer. CV measurements were carried out at a scan rate of 1 V s^{-1}, in the potential range from −800 to 0 mV in the measurement buffer, 50 mM phosphate buffer (pH 7) containing 150 mM NaCl. The measurement solution was degassed with pure N_2 for 30 min prior to experiments. Importantly, all measurements were repeated for a minimum of three times with separate electrodes to obtain statistically meaningful results.

Optimization of the Number and Position of MB Molecules. A set of nine sensors were prepared and each sensor was incubated with a mixture of 7.5 μL of 1 μM strand C (miR-122-5p), 7.5 μL of 1 μM strand H (miR-122-5p), and 15 μL of 2 μM miR-122-5p in the incubation buffer, for 1 h at 37 °C in a dark humidity chamber.

To simplify, the number following the adaptor strand letter denotes the number of methylene blue (MB) molecules attached to the strand; for example, C1 indicates that the C adaptor strand is modified at one end with 1 MB molecule. Eight combinations of the adaptor strands and miR-122-5p were tested, including C1H0, C2H0, C0H1, C0H2, C1H1, C2H1, C1H2, and C2H2. A control experiment was carried out using a mixture of the nonlabeled adaptor strands C0 and H0 and the target miRNA.

Serum miRNAs Extraction. Human serum samples were purchased from Bioreclamation Inc., U.S. and include (1) sera from normal male and female donors (pooled), (2) B-cell chronic lymphocytic leukemia sera of a Caucasian, 65 years old, female donor with disease stage Rai III, and (3) B-cell chronic lymphocytic leukemia sera of a Caucasian, 70 years old, male donor with disease stage Rai I. No information about the treatment outcome was supplied with the sample. All samples were kept at −80 °C until ready to use. Next, 300 μL of each human serum (normal and both CLL) was thawed on ice and mixed by inverting. Circulating miRNAs were isolated from all samples using miRCURY RNA Isolation kit−Biofluids (Exiqon, Denmark), according to the manufacturer's protocol with the

DOI: 10.1021/ac504331c
Anal. Chem. 2015, 87, 1395−1403

following modifications. Briefly, 7 fM synthetic *Caenorhabditis elegans* miRNA (Cel-miR-39-3p) was added to each sample to monitor the efficiency of miRNA extraction and allow for normalization of sample-to-sample variation. The synthetic miRNA was added after denaturation of the sample, to avoid its degradation by endogenous serum RNases. Afterward, 60 μL of the lysis solution was added to each serum sample and the sample was lysed by vortexing followed by incubation for 3 min at room temperature. Next, 1 μL of synthetic cel-miR-39 was added to each lysate fraction. Then, 20 μL of protein precipitation solution was added and mixed by vortexing followed by incubation for 1 min at room temperature. Afterward, the mixture was centrifuged for 3 min at 11000*g* and the supernatant was transferred into a new collection tube. After 270 μL of isopropyl alcohol was added, the sample was loaded onto a microRNA mini spin column followed by incubation for 2 min at room temperature then spun down. After the bound RNAs were washed for three times, the RNAs were eluted in 75 μL of RNase free water. Purified RNAs were kept at −80 °C until ready to use.

Electrochemical Profiling of miRNAs in Serum. Serum miRNAs were measured twice; first in the serum extract obtained from the previous step and second in the serum directly after proper treatment.

For miRNA profiling in the serum extract, 16 sensors were prepared as, previously discussed in the Sensor Preparation section. Next, each set of 4 isolated quadrants was utilized for detection of a specific miRNA in normal healthy serum, chronic lymphocytic leukemia Rai stage 1 (CLL-1), and Rai stage 3 (CLL-3) sera, and in the incubation buffer as a control. This was accomplished by incubating each sensor with a mixture of 1 μM C2 and H2 adaptor strands specific to the tested miRNA (7.5 μL each) and 15 μL of 1/100 dilution of the serum extract for 1 h at 37 °C in a dark humidity chamber. Subsequently, CV was performed in a solution of 10 μM glucose oxidase in the measurement buffer. The developed four sets of sensors were utilized for profiling of miR-16-5p, miR-21-5p, miR-150-5p, and the internal standard, cel-miR-39-3p, using the respective adaptor strands specific for each miRNA. For miRNA profiling in serum directly, 20 sensors were prepared. Afterward, 100 μL of 100 μM 2-mercaptoethanol (Sigma-Aldrich, U.S.) was added to 100 μL of each serum sample and the volume was completed to 990 μL using the incubation buffer. This was followed by heating each aliquot for 15 min at 95 °C. Afterward, 10 μL of 100 pM internal standard was added to each aliquot.

Subsequently, 15 μL of each aliquot was mixed with the specific adaptor strands and incubated with the sensor for 1 h at 37 °C in a dark humidity chamber. A control experiment was performed by incubating the developed sensors with 15 μL of 5.1 mg mL^{-1} human serum albumin (HSA, Sigma-Aldrich, U.S.) in the incubation buffer in the presence of the respective adaptor strands. Another control experiment was carried out by incubating the developed sensors with 1 μM UIP complement for 1 h at 37 °C. This was followed by incubation with the normal serum aliquot in the presence of the respective adaptor strands. Subsequently, CV measurement was performed in 10 μM glucose oxidase solution in the measurement buffer.

Quantitative RT-PCR of Mature miRNAs. A fixed volume of 4 μL of RNA solution from the RNA isolation sample was used as an input for the reverse transcription (RT) reaction. For generation of standard curves, synthetic RNA oligonucleotides corresponding to known miRNAs were used. Several aliquots of each synthetic miRNA were made in nuclease free water such that the final input into the RT reaction had a volume of 4 μL. The miRNA was reverse transcribed using a miRCURY LNA Universal RT miRNA PCR kit and miRNA-specific LNA primer set (Exiqon, Denmark). The 19 μL RT reaction consists of 4 μL of 5× reaction buffer, 9 μL of nuclease free H_2O, 2 μL of the enzyme mix, and 4 μL of the input RNA. For nontemplate control, nuclease free water was used. Synthetic UniSP6 RNA spike-in oligonucleotide was added to each RT reaction, to monitor the cDNA synthesis reaction for signs of inhibition. All the components, other than the RNA, were prepared as a larger volume master mix. The RT reaction was performed using a thermal cycler (Mastercycler pro S, Eppendorf, Germany) at 42 °C for 60 min and 95 °C for 5 min followed by immediate cooling at 4 °C.

The reverse transcription reaction products were diluted 40 times in nuclease free water and 4 μL of the aliquot were combined with 5 μL of SYBRGreen master mix and 1 μL of PCR primer mix (Exiqon, Denmark) to generate a PCR reaction of 10 μL. Real-time PCR was carried out on a Bio-Rad CFX thermocycler at 95 °C for 10 min, followed by 40 cycles of 95 °C for 10 s and 60 °C for 1 min. An additional step in the qRT-PCR analysis was performed to evaluate the specificity of the assays by generating a melting curve for each reaction. Obtained data were analyzed using CFX manager software version 3.0 (Bio-Rad, U.S.), with automated assay-specific baseline and threshold settings.

Quantification of miRNAs by qRT-PCR. Starting with a 200 pM solution of synthetic miR-16-5p corresponding to the mature sequence (miRBase release 19, August 2012), a primary dilution of 40 pM was made by adding 4 μL of the solution to 16 μL of nuclease free water. From this initial dilution, 10 serial 4-fold dilutions were made. The qRT-PCR of synthetic miRNA aliquots was run in parallel with experimental serum samples. In order to avoid cross-contamination of the serum samples with the highly concentrated synthetic oligonucleotide dilutions, experimental serum samples were separated by two empty rows during the RT and real-time PCR reaction. The Ct values were plotted against the logarithmic starting concentration of synthetic miR-16-5p in a standard curve. It is worth noting that there is no established housekeeping miRNA control for normalization of technical variations in sample processing. Thus, the data normalization was carried out using a nonhuman synthetic miRNA, cel-miR-39-3p, which was spiked-in after denaturing the serum sample. As described earlier, the level of cel-miR-39 was measured in each serum sample using SYBR Green qRT-PCR assays (Bio-Rad, U.S.).

RESULTS AND DISCUSSION

Principle of the Sens^{PEQ}. This is a multicomponent sensor that consists of a thiol modified universal interfacial probe (UIP) and two DNA adaptor strands, namely strand C and strand H, which cooperatively hybridize with both the UIP and the target miRNA. The adaptor strands are labeled at both ends with methylene blue (MB), which has a characteristic redox signal. Each adaptor strand has a fragment complementary to the UIP (UIP-binding arm) and a fragment complementary to the analyzed miRNA (miRNA-binding arm). In absence of the target miRNA, the adaptor strands do not interact with the surface-bound UIP, because the UIP stem−loop structure is thermodynamically more stable than its associate with the adaptor strands. Also, the adaptor strands are designed with a short UIP-binding arm to prevent their hybridization with the detection probe in absence of the target. In the presence of

DOI: 10.1021/ac504331c
Anal. Chem. 2015, 87, 1395−1403

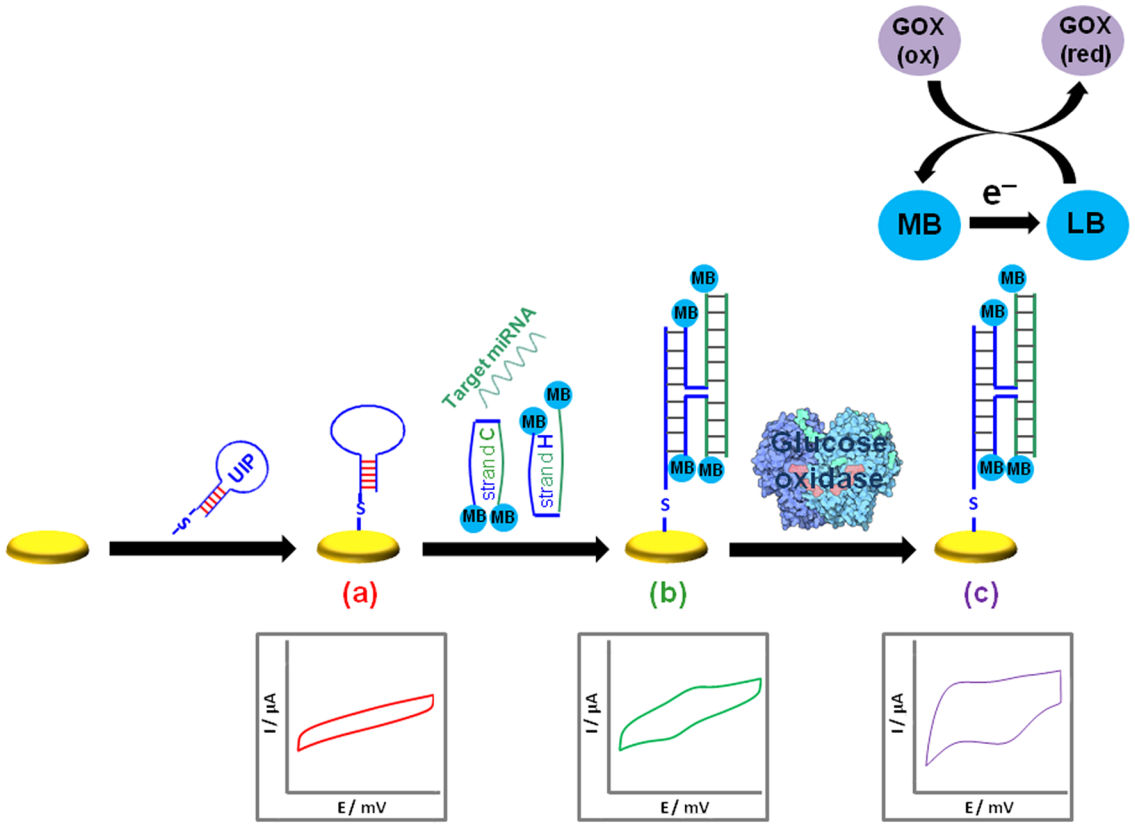

Figure 1. Schematic representation of a protein-facilitated electrocatalytic quadroprobe sensor ($Sens^{PEQ}$) for detection of microRNAs. (a) Thiol-modified universal interfacial probe (UIP) was self-assembled onto the electrode surface followed surface backfilling with 2-mercaptohexanol. (b) Incubation of the sensor with a mixture of the target microRNA and the methylene blue (MB) labeled adaptor strands, namely C and H strands, results in the formation of a characteristic redox peak measured by cyclic voltammetry (CV). (c) CV in the presence of glucose oxidase showing the amplification of the MB reductive peak resulting from electrocatalysis.

miRNA, the two adaptor strands will hybridize with the UIP and the target miRNA to form a quadripartite complex with a four-way junction structure. The formation of the complex can be detected by measuring the MB characteristic redox signal with cyclic voltammetry (CV). The presence of four MB molecules in the formed complex with the target miRNA significantly amplifies the signal and the corresponding sensor is called quadroprobe-based sensor, $Sens^{Q}$. Furthermore, protein electrocatalysis is performed to further enhance the overall signal gain and thus came the name protein-facilitated electrocatalytic quadroprobe sensor, $Sens^{PEQ}$. A schematic representation of the proposed $Sens^{PEQ}$ is shown in Figure 1.

Effect of the Number and Position of MB Molecules on the Sensor Response. In this work, 10 mM $MgCl_2$ was included in the incubation buffer to screen the negative charge of the sugar phosphate backbone of DNA, allowing the formation of a densely packed DNA monolayer.[53] Prior to electrochemical analysis, eight combinations of the adaptor strands and miR-122-5p were formed, including C1H0, C2H0, C0H1, C0H2, C1H1, C2H1, and C1H2, whereas C0H0 was used as a control. As can be seen in Figure 2A,B, larger reduction currents were obtained using C1H0 and C2H0 compared to C0H1 and C0H2, respectively. This might be attributed to the ease of direct surface reduction of proximal MB molecules compared to their distal counterparts. The presence of four MB molecules in the formed four-way junction based hybrid caused the largest increase in the reductive signal. Thus, the $Sens^{Q}$ was utilized for further experiments. Interestingly, the presence of two adjacent MB molecules in C0H2 and C2H0 had a synergistic effect on the overall signal gain. Admittedly, the reason for such observation is still unclear due to the novelty of the proposed multiprobe sensing platform.

$Sens^{Q}$ for miRNA Analysis. Prior to titration experiments, aliquots containing different concentrations of miR-122-5p ranging from 2 fM to 2 μM in 15 μL of the incubation buffer were mixed with 1 μM C2 and H2 adaptor strands (7.5 μL each) and the mixture was incubated with the UIP-modified electrode using the same experimental conditions. A control experiment was performed using the incubation buffer alone instead of miRNA. It was observed that the developed sensor is capable of detecting miR-122-5p down to 100 fM ($\sim 6 \times 10^4$ molecules/μL). Also, the ability of $Sens^{Q}$ to detect single base mismatches in the target strand was tested with reference to incubation with 100 fM perfectly matched (PM) miR-122-5p in the mixture (33.1 nC, 100%) and the control (6.1 nC, 0%). It was observed that the presence of a terminal base mismatch (T-SMBc) in the C allele caused a 83.9% increase in the reductive peak area (28.7 nC). On the other hand, larger signal attenuation was observed in the presence of a middle single base mismatch in the C allele (M-SBMc, 15.9 nC, 36.3%) and U allele (M-SBMu, 12.8 nC, 24.7%), as shown in Figure 2C and 2D. This might be attributed to the lower hybridization efficiency of the mismatch containing strand.[32]

In an attempt to further enhance the sensor sensitivity, five different electrodes were tested for detection of 15 μL of 2 μM

DOI: 10.1021/ac504331c
Anal. Chem. 2015, 87, 1395−1403

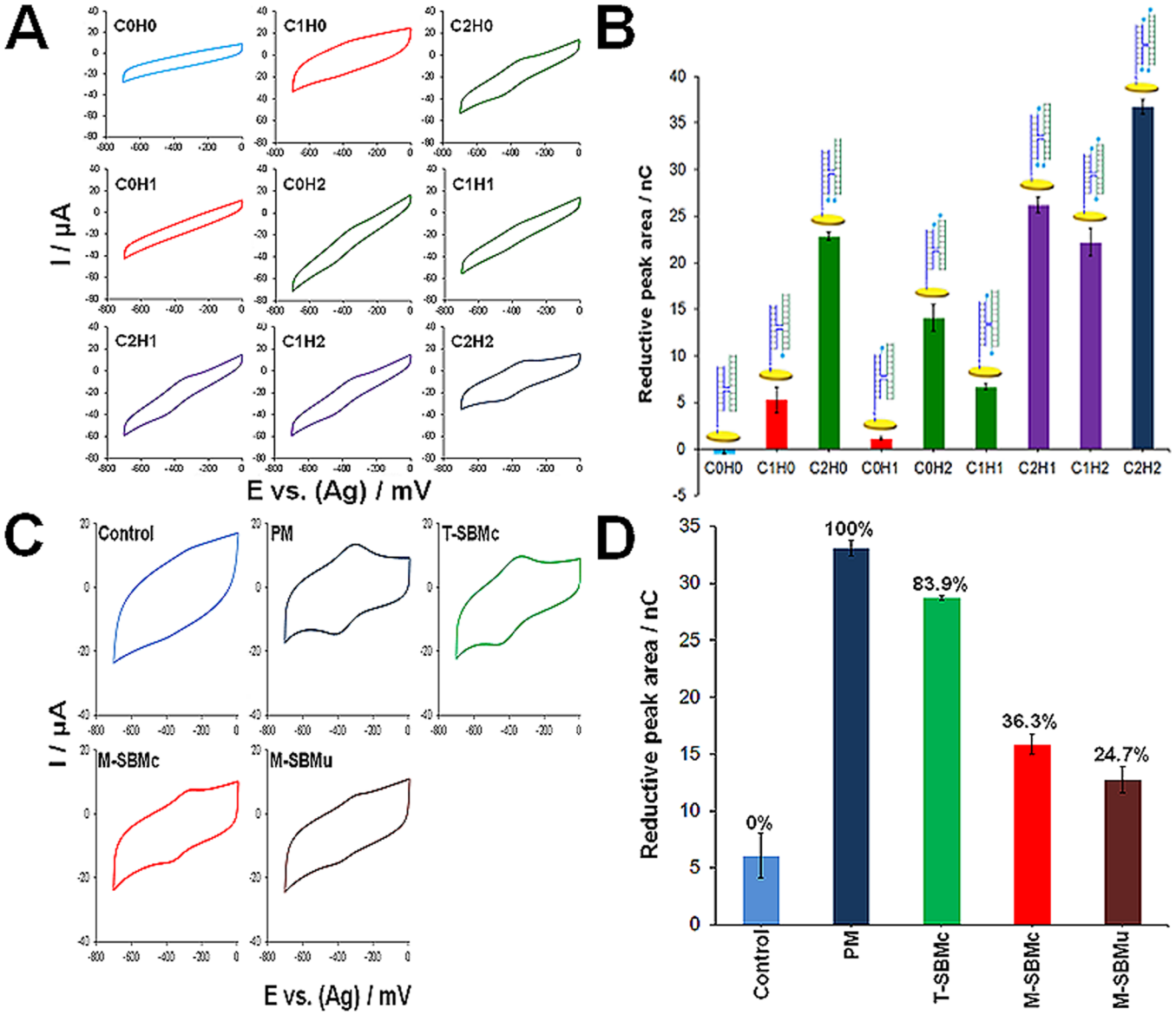

Figure 2. Effect of the number and position of MB molecules on the sensor sensitivity and selectivity. (A) Cyclic voltammograms of the developed electrochemical sensors showing the effect of the number and position of methylene blue (MB) molecules in the C and H adaptor strands on the redox current intensity. Eight combinations were tested, including C1H0, C2H0, C0H1, C0H2, C1H1, C2H1, C1H2, and C2H2. A control experiment was performed using the non labeled adaptor strands, C0H0. (B) Plot of the MB reductive peak area vs the tested combinations of adaptor strands. A blue dot represents methylene blue. (C) Cyclic voltammograms of the developed electrochemical sensors obtained using 100 fM perfectly matched (PM) miR-122-5p and C alleles containing a terminal base mismatch (T-SBMc) and middle single base mismatch (M-SBMc), and a U allele with middle single base mismatch (M-SBMu). A control experiment was performed by incubating the sensor with the incubation buffer alone in the presence of the adaptor strands. (D) Plot of the MB reductive peak area vs the type of the utilized miRNA.

miR-122-5p, using a mixture of 1 μM C2 and H2 adaptor strands (7.5 μL each) under the same experimental conditions. The tested electrodes comprised a screen-printed gold electrode (SPGE) and gold nanoparticles-modified graphene (GNPs-GPH), gold nanoparticles–carbon nanofibers (GNPs-CNFs), gold nanoparticles–screen printed carbon electrode (GNPs-SPCE), and gold nanoparticles–carbon nanotubes (GNPs-CNTs). As shown in Figure 3A,B, it was observed that the maximum reductive signal was obtained with the GNPs-GPH and hence it was selected for further experiments.

Enhancement of Sens^{Q} Response Using Electrocatalysis. We attempted to utilize the developed Sens^{Q} for profiling of hsa-miR-16-5p, hsa-miR-21-5p, and hsa-miR-150-5p in 1/100 dilution of the RNA extract obtained from human normal serum, CLL-1, and CLL-3, in the presence of *cel*-miR-39 as an internal standard. Unfortunately, it was noticed that Sens^{Q} lacks the sufficient sensitivity to provide a significant response for the analyzed miRNAs (unpublished data). Therefore, we resorted to integrate electrocatalysis into the developed sensor and the respective Sens^{PEQ} was utilized for further experiments. It is well established that electrocatalysis represents the preferred means of signal amplification in electrochemical sensing.[54] The degree of electroctalytic signal amplification depends upon the rigorous shielding of the electron sink from the electrode surface, which prevents the direct reduction of the electrocatalyst by the electrode and false positive outputs.[55] In addition, the reporter must interact with both the base stack and the freely diffusing electron sink.[56] A

DOI: 10.1021/ac504331c
Anal. Chem. 2015, 87, 1395–1403

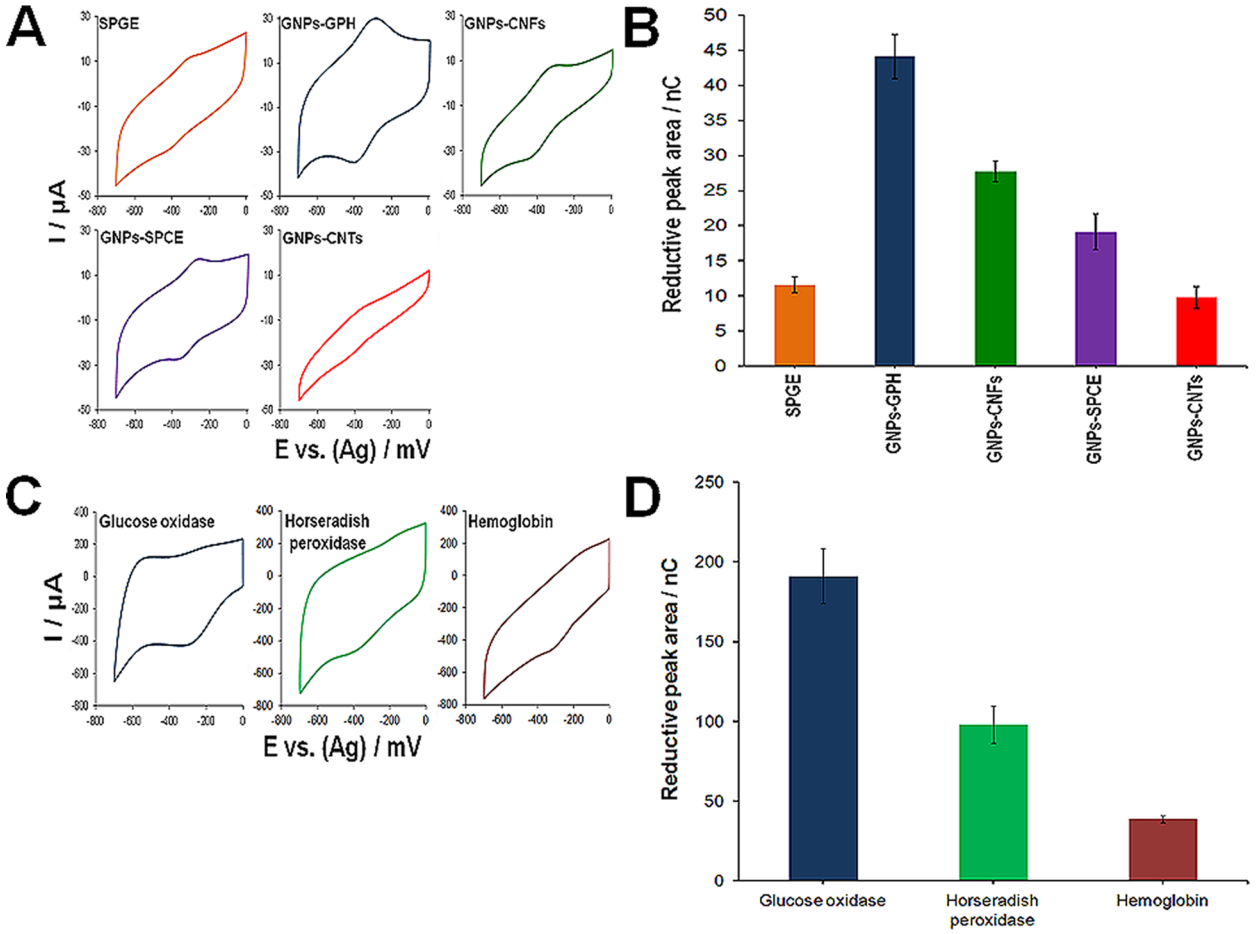

Figure 3. Effect of the sensor material and electrocatalyst on the assay sensitivity. (A) Cyclic voltammograms of the developed electrochemical sensors showing the effect of the electrode material on the redox current intensity. Five electrodes were tested, including a screen-printed gold electrode (SPGE) and gold nanoparticles−modified graphene (GNPs-GPH), −carbon nanofibers (GNPs-CNFs), −screen printed carbon electrode (GNPs-SPCE), and −carbon nanotubes (GNPs-CNTs). (B) Plot of the MB reductive peak area vs the electrode type. (C) Cyclic voltammograms of the developed electrochemical sensors showing the effect of the electrocatalyst on the reduction current intensity. Three electrocatalysts were tested, including glucose oxidase, horseradish peroxidase, and hemoglobin. (D) Plot of the MB reductive peak area vs the type of the utilized electrocatalyst.

previous attempt at electrocatalysis employed negatively charged functionalized mercaptoalkanes to shield electrocatalysts of small molecular mass, e.g., ferricyanide, from the electrode surface.[57] However, this platform has not been widely accepted due to the difficulty of imposing a sufficient kinetic barrier to the reduction of ferricyanide required to drive electrocatalysis. Redox-active proteins such as glucose oxidase and horseradish peroxidase have been shown to readily interact with phenothiazine dyes such as Nile blue, and have had many applications as recognition elements in sensing devices. Also, hemoglobin exhibits the same feature and has been shown to couple with Nile blue.[58] Detection platforms based on these redox-active proteins are appealing due to their inherent catalytic activity. In addition, the application of a protein as an electron sink is highly attractive due to the ability of the protein shell to shield the redox core from the electrode surface. In this work, three different electrocatalysts were tested for detection of 15 μL of 2 μM miR-122-5p, using a mixture of 1 μM C2 and H2 adaptor strands (7.5 μL each) under the same experimental conditions. The tested electrocatalysts included glucose oxidase, horseradish peroxidase, and hemoglobin (10 μM each). Admittedly, we could not obtain a significant electrocatalytic signal using the GNPs-GPH that formerly provided the largest signal with the $Sens^{Q}$ system. This might be attributed to the nature of the electrode material that consists of gold nanoparticles (GNPs) doped into an electrochemically active carbon matrix. Hence, some extent of direct surface reduction of the electrocatalyst might have occurred at the vacant carbon matrix. Therefore, SPGEs were utilized for further experiments. As shown in Figure 3C, the electrocatalytic signal amplification is apparent in the CV by the characteristic nonreversible redox signal, where the reductive peak is amplified and the oxidative peak is abolished. This could be ascribed to the two-electron reduction of MB to leucomethylene blue (LB) that subsequently decreases the binding affinity of the reporter to the base stack, resulting in its dissociation from the duplex. Then, LB electrochemically interacts with, and reduce two equivalents of the electrocatalyst, returning the reporter to the oxidized state and allowing for repeated integration of the reporter into the base stack to complete the electrocatalytic cycle. As shown in Figure 3C,D, it was observed that the maximum reductive signal was obtained with glucose oxidase and hence it was utilized for serum experiments.

$Sens^{PEQ}$ for miRNA Profiling in Serum. The developed $Sens^{PEQ}$ was utilized for profiling of three endogenous CLL specific miRNAs including, hsa-miR-16-5p, hsa-miR-21-5p, and hsa-miR-150-5p, in addition to the internal standard *cel*-miR-39,

DOI: 10.1021/ac504331c
Anal. Chem. 2015, 87, 1395−1403

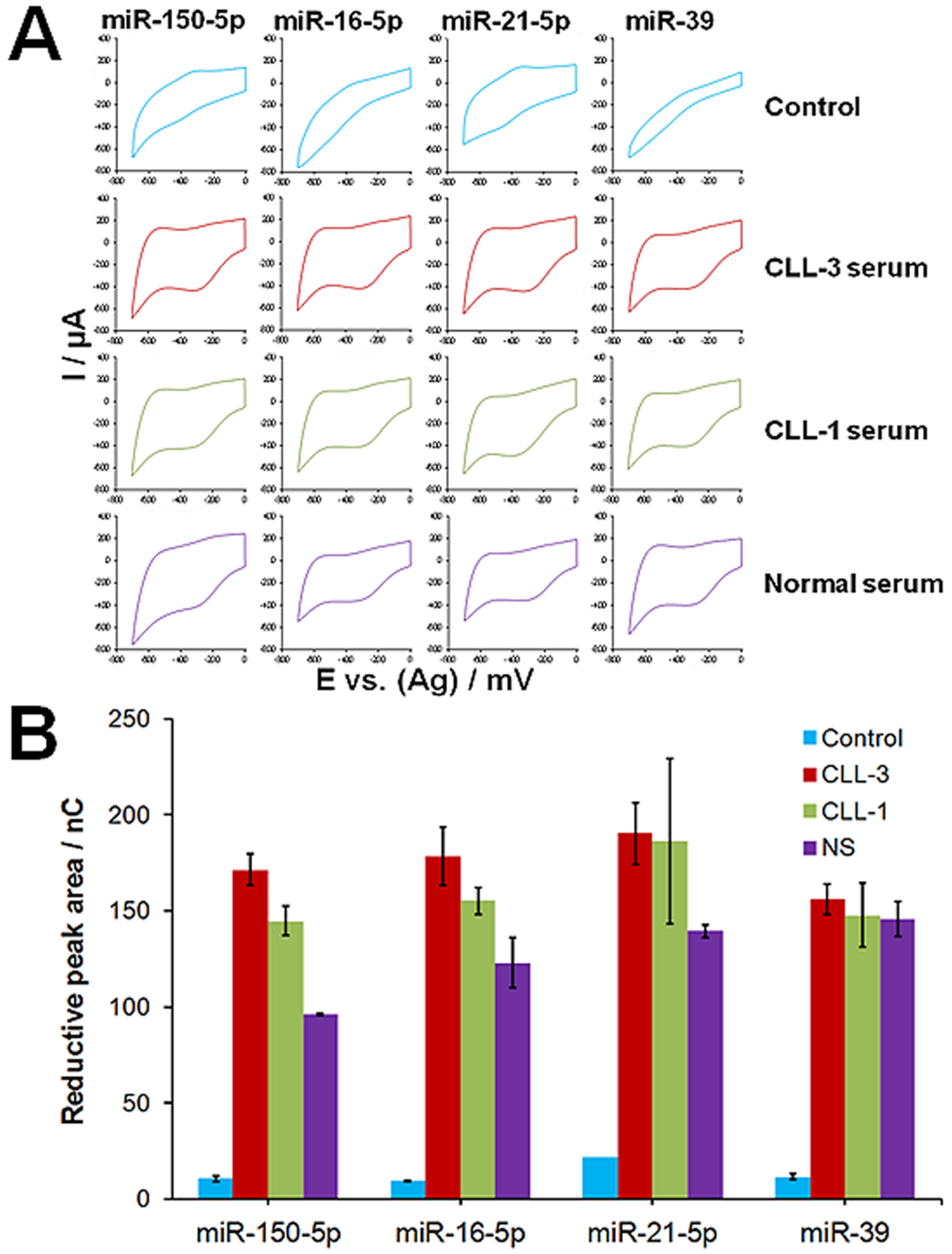

Figure 4. Sens^{PEQ} for miRNA profiling in serum extract. (A) Cyclic voltammograms of the developed electrochemical sensors developed for detection of miR-16-5p, miR-21-5p, miR-150-5p, and the internal standard, miR-39, in normal healthy serum, chronic lymphocytic leukemia Rai stage 1 (CLL-1), and Rai stage 3 (CLL-3) sera. Control experiments were performed by incubating the developed sensors with the incubation buffer alone in the presence of the adaptor strands. (B) Plot of the MB reductive peak area vs the type of the miRNA analyzed in each serum.

in the RNA extract of normal serum, CLL-1, and CLL-3 sera, using the incubation buffer as a control. As can be seen in Figure 4A,B, it was observed that the three endogenous miRNAs have exhibited an increased expression of varying degrees, in the CLL-3 serum compared to CLL-1 and healthy serum. The results were normalized by subtraction of the background signal caused by the adaptor strands in buffer. This was followed by calculation of the fold changes relative to the internal standard and the normalized values are presented in Figure 5A. In an attempt to verify the results, the developed sensor was utilized for profiling of the same endogenous miRNAs, in addition to the internal standard, directly in the serum samples after treatment with 2-mercaptoethanol to inhibit the ribonucleases followed by heating to release the miRNAs from the circulating exosomes. Two control experiments were carried out, including incubating the developed sensors with 5.1 mg mL^{-1} HSA in the incubation buffer in the presence of the respective adaptor strands. Another control experiment was carried out by incubating the developed sensors with the UIP complement followed by incubation with the normal serum aliquot in the presence of the respective adaptor strands. As shown in Figure S1A,B (Supporting Information), quite similar trends were obtained with slight variations. The results were normalized by calculation of the fold changes relative to the internal standard and the normalized values are presented in Figure 5B. For further verification of the Sens^{PEQ} results, qRT-PCR was utilized for analysis of the CLL specific endogenous miRNAs in the presence of the internal standard.

DOI: 10.1021/ac504331c
Anal. Chem. 2015, 87, 1395−1403

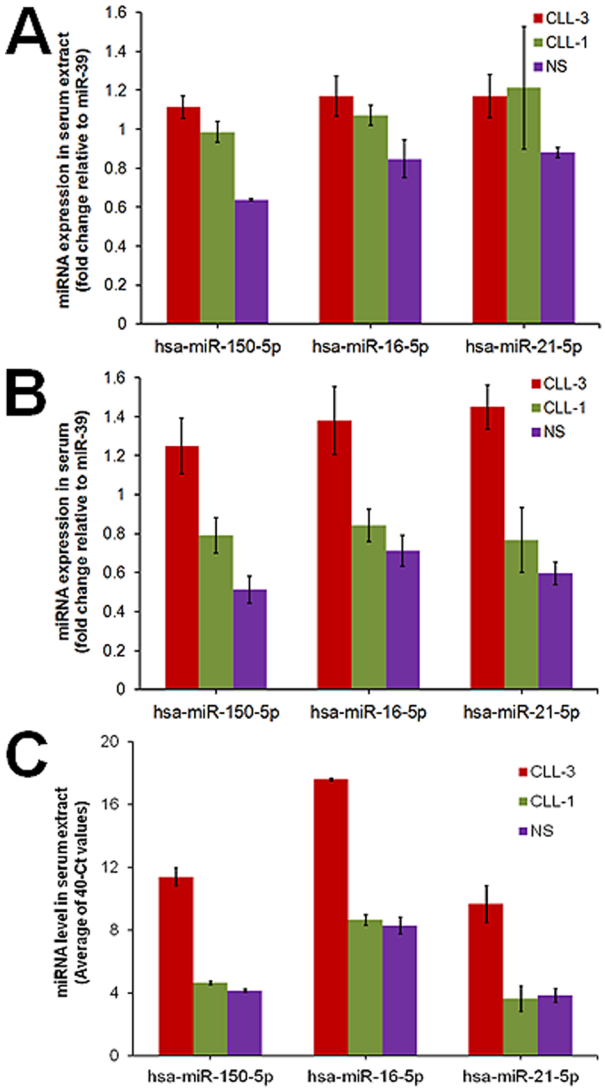

Figure 5. Sens^{PEQ} and qRT-PCR for miRNA profiling in serum. Plot of the expression profile of three miRNAs, including miR-150, miR-16, and miR-21 in (A) extracted and (B) crude normal healthy serum (NC), chronic lymphocytic leukemia Rai stage 1 (CLL-1), and Rai stage 3 (CLL-3) sera relative to the internal standard miR-39. (C) MicroRNA levels in normal healthy serum and different stages of CLL serum samples obtained by qRT-PCR. Values presented here, represent the average of three replicate of RT reactions followed by real-time PCR. Ct values were normalized by using measurements of spiked-in synthetic normalization control, *cel*-miR-39 that was introduced to the sample during RNA isolation.

qRT-PCR for miRNA Analysis. We investigated three blood-based miRNA biomarker candidates for CLL based on published miRNA expression profiling data. These miRNAs were analyzed in three serum aliquots of the CLL-3, CLL-1, and a healthy pooled control sample. The RNAs were isolated from the three samples and screened for differential expression of these miRNAs by SYBR Green qRT-PCR assays. The results indicated that these miRNAs showed increased expression of varying degrees, in the CLL-3 serum compared to CLL-1 and healthy control serum, as shown in Figure 5C. Of all three candidates, the level of miR-16-5p was the highest in CLL-3 sample. The involvement of miR-16 in the pathogenesis of CLL was previously reported by Klein et al.[46] As can be seen in Figure 5A,B,C, a similar miRNA profile was obtained by both the Sens^{PEQ} and qRT-PCR with slight variations in the level of each miRNA. This is presumably due to the variation in the reactivity of each miRNAs during the polyadenilation, reverse transcription, and amplification steps in qPCR experiments. In addition, the CV method adopted in this study relies on baseline integration for measuring the reductive peak area. Taking into account the relatively large background current created by four surface attached MB molecules, hence a small degree of error in reductive area calculations cannot be excluded.

CONCLUSIONS

Implementation of commercially available electrochemical sensors in clinical diagnostics requires highly sensitive and selective techniques. The developed protein-facilitated electrocatalytic quadroprobe sensor (Sens^{PEQ}) allows instantaneous ultrasensitive profiling of miRNAs directly in serum. The indirect binding of the detection probe to the target makes this approach readily adaptable for analysis of any given miRNA by simple replacement of the miRNA-binding arms of the adaptor strands. A novel means to improve the overall signal-ON gain of the developed sensor is demonstrated using a compatible combination of two DNA adaptor strands modified with four methylene blue molecules and electrocatalysis using glucose oxidase. As an electron sink, glucose oxidase is effective in physiologically relevant pH ranges and, as a compact protein, it cannot be directly reduced at the sensor surface, thus minimizing false positives. This enhanced sensitivity provided the response necessary to detect the low-abundant circulating miRNAs without preamplification. The proposed sensing platform might be useful for the fabrication of signal-ON multiprobe optical sensors for miRNA analysis by simply replacing the MB molecules with fluorophores. Also, the developed technique is applicable to many electrochemical sensing strategies based on redox reporting of MB. In addition, the developed Sens^{PEQ} is exquisitely sensitive to intervening π-stack perturbations and capable of distinguishing single base mismatches in the target miRNA. Furthermore, the developed sensor is based on cheap and commercially available electrodes. This is foreseen to open a new venue for the large-scale production of disposable one-shot miRNA POCs with significant impact on early diagnosis of many diseases and forensic analysis of body fluids.

ASSOCIATED CONTENT

Supporting Information

Sequence of the nucleic acids utilized in the experimental setup and Sens^{PEQ} for miRNA profiling in serum. This material is available free of charge via the Internet at http://pubs.acs.org.

AUTHOR INFORMATION

Corresponding Author

*M. V. Berezovski. E-mail: maxim.berezovski@uottawa.ca.

Notes

The authors declare no competing financial interest.

ACKNOWLEDGMENTS

The authors thank the Mitacs Elevate Fellowship Program (M.L.) and the Natural Sciences and Engineering Research Council of Canada (M.V.B.) for funding this work.

DOI: 10.1021/ac504331c
Anal. Chem. 2015, 87, 1395−1403

REFERENCES

(1) Ambros, V. *Nature* **2004**, *431*, 350−355.
(2) Bartel, D. P. *Cell* **2004**, *116*, 281−297.
(3) Lu, J.; Getz, G.; Miska, E. A.; Alvarez-Saavedra, E.; Lamb, J.; Peck, D.; Sweet-Cordero, A.; Ebert, B. L.; Mak, R. H.; Ferrando, A. A.; Downing, J. R.; Jacks, T.; Horvitz, H. R.; Golub, T. R. *Nature* **2005**, *435*, 834−838.
(4) Boon, R. A.; Iekushi, K.; Lechner, S.; Seeger, T.; Fischer, A.; Heydt, S.; Kaluza, D.; Treguer, K.; Carmona, G.; Bonauer, A.; Horrevoets, A. J.; Didier, N.; Girmatsion, Z.; Biliczki, P.; Ehrlich, J. R.; Katus, H. A.; Muller, O. J.; Potente, M.; Zeiher, A. M.; Hermeking, H.; Dimmeler, S. *Nature* **2013**, *495*, 107−110.
(5) Miller, B. H.; Wahlestedt, C. *Brain Res.* **2010**, *1338*, 89−99.
(6) Pandey, A. K.; Agarwal, P.; Kaur, K.; Datta, M. *Cell Physiol. Biochem.* **2009**, *23*, 221−232.
(7) Lodes, M. J.; Caraballo, M.; Suciu, D.; Munro, S.; Kumar, A.; Anderson, B. *PLoS One* **2009**, *4*, e6229.
(8) Zen, K.; Zhang, C.-Y. *Med. Res. Rev.* **2012**, *32*, 326−348.
(9) Catuogno, S.; Esposito, C. L.; Quintavalle, C.; Cerchia, L.; Condorelli, G.; De Franciscis, V. *Cancers (Basel)* **2011**, *3*, 1877−1898.
(10) Varallyay, E.; Burgyan, J.; Havelda, Z. *Nat. Protoc.* **2008**, *3*, 190−196.
(11) de Planell-Saguer, M.; Rodicio, M. C.; Mourelatos, Z. *Nat. Protoc.* **2010**, *5*, 1061−1073.
(12) Volinia, S.; Calin, G. A.; Liu, C. G.; Ambs, S.; Cimmino, A.; Petrocca, F.; Visone, R.; Iorio, M.; Roldo, C.; Ferracin, M.; Prueitt, R. L.; Yanaihara, N.; Lanza, G.; Scarpa, A.; Vecchione, A.; Negrini, M.; Harris, C. C.; Croce, C. M. *Proc. Natl. Acad. Sci. U. S. A.* **2006**, *103*, 2257−2261.
(13) Livak, K. J.; Schmittgen, T. D. *Methods* **2001**, *25*, 402−408.
(14) Thomas, M. F.; Ansel, K. M. *Methods Mol. Biol.* **2010**, *667*, 93−111.
(15) Klein, D. *Trends Mol. Med.* **2002**, *8*, 257−260.
(16) Hafner, M.; Landgraf, P.; Ludwig, J.; Rice, A.; Ojo, T.; Lin, C.; Holoch, D.; Lim, C.; Tuschl, T. *Methods* **2008**, *44*, 3−12.
(17) Fang, S.; Lee, H. J.; Wark, A. W.; Corn, R. M. *J. Am. Chem. Soc.* **2006**, *128*, 14044−14046.
(18) Driskell, J. D.; Seto, A. G.; Jones, L. P.; Jokela, S.; Dluhy, R. A.; Zhao, Y. P.; Tripp, R. A. *Biosens. Bioelectron.* **2008**, *24*, 923−928.
(19) Cissell, K. A.; Rahimi, Y.; Shrestha, S.; Hunt, E. A.; Deo, S. K. *Anal. Chem.* **2008**, *80*, 2319−2325.
(20) Neely, L. A.; Patel, S.; Garver, J.; Gallo, M.; Hackett, M.; McLaughlin, S.; Nadel, M.; Harris, J.; Gullans, S.; Rooke, J. *Nat. Methods* **2006**, *3*, 41−46.
(21) Wang, J.; Yi, X.; Tang, H.; Han, H.; Wu, M.; Zhou, F. *Anal. Chem.* **2012**, *84*, 6400−6406.
(22) Labib, M.; Zamay, A. S.; Kolovskaya, O. S.; Reshetneva, I. T.; Zamay, G. S.; Kibbee, R. J.; Sattar, S. A.; Zamay, T. N.; Berezovski, M. V. *Anal. Chem.* **2012**, *84*, 8966−8969.
(23) Labib, M.; Zamay, A. S.; Muharemagic, D.; Chechik, A. V.; Bell, J. C.; Berezovski, M. V. *Anal. Chem.* **2012**, *84*, 1813−1816.
(24) Labib, M.; Zamay, A. S.; Kolovskaya, O. S.; Reshetneva, I. T.; Zamay, G. S.; Kibbee, R. J.; Sattar, S. A.; Zamay, T. N.; Berezovski, M. V. *Anal. Chem.* **2012**, *84*, 8114−8117.
(25) Labib, M.; Zamay, A. S.; Muharemagic, D.; Chechik, A.; Bell, J. C.; Berezovski, M. V. *Anal. Chem.* **2012**, *84*, 1677−1686.
(26) Labib, M.; Zamay, A. S.; Muharemagic, D.; Chechik, A.; Bell, J. C.; Berezovski, M. V. *Anal. Chem.* **2012**, *84*, 2584−2586.
(27) Labib, M.; Zamay, A. S.; Berezovski, M. V. *Analyst* **2013**, *138*, 1865−1875.
(28) Labib, M.; Martić, S.; Shipman, P. O.; Kraatz, H. B. *Talanta* **2011**, *85*, 770−778.
(29) Labib, M.; Shipman, P. O.; Martić, S.; Kraatz, H. B. *Electrochim. Acta* **2011**, *56*, 5122−5128.
(30) Labib, M.; Shipman, P. O.; Martić, S.; Kraatz, H. B. *Analyst* **2011**, *136*, 708−715.
(31) Labib, M.; Khan, N.; Ghobadloo, S. M.; Cheng, J.; Pezacki, J. P.; Berezovski, M. V. *J. Am. Chem. Soc.* **2013**, *135*, 3027−3038.
(32) Labib, M.; Ghobadloo, S. M.; Khan, N.; Kolpashchikov, D. M.; Berezovski, M. V. *Anal. Chem.* **2013**, *85*, 9422−9427.
(33) Wang, J.; Liu, G.; Merkoci, A. *J. Am. Chem. Soc.* **2003**, *125*, 3214−3215.
(34) Peng, Y.; Yi, G.; Gao, Z. *Chem. Commun. (Cambridge, U. K.)* **2010**, *46*, 9131−9133.
(35) Gao, Z.; Yu, Y. H. *Biosens. Bioelectron.* **2007**, *22*, 933−940.
(36) Lusi, E. A.; Passamano, M.; Guarascio, P.; Scarpa, A.; Schiavo, L. *Anal. Chem.* **2009**, *81*, 2819−2822.
(37) Fan, Y.; Chen, X.; Trigg, A. D.; Tung, C. H.; Kong, J.; Gao, Z. *J. Am. Chem. Soc.* **2007**, *129*, 5437−5443.
(38) Yang, H.; Hui, A.; Pampalakis, G.; Soleymani, L.; Liu, F. F.; Sargent, E. H.; Kelley, S. O. *Angew. Chem., Int. Ed. Engl.* **2009**, *48*, 8461−8464.
(39) Gao, Z.; Yang, Z. *Anal. Chem.* **2006**, *78*, 1470−1477.
(40) Peng, Y.; Gao, Z. *Anal. Chem.* **2011**, *83*, 820−827.
(41) Qavi, A. J.; Kindt, J. T.; Bailey, R. C. *Anal. Bioanal. Chem.* **2010**, *398*, 2535−2549.
(42) Tsimberidou, A. M.; Keating, M. J. *Cancer* **2009**, *115*, 2824−2836.
(43) Rai, K. R.; Sawitsky, A.; Cronkite, E. P.; Chanana, A. D.; Levy, R. N.; Pasternack, B. S. *Blood* **1975**, *46*, 219−234.
(44) Binet, J. L.; Vaugier, G.; Dighiero, G.; d'Athis, P.; Charron, D. *Am. J. Med.* **1977**, *63*, 683−688.
(45) Moussay, E.; Wang, K.; Cho, J. H.; van Moer, K.; Pierson, S.; Paggetti, J.; Nazarov, P. V.; Palissot, V.; Hood, L. E.; Berchem, G.; Galas, D. J. *Proc. Natl. Acad. Sci. U. S. A.* **2011**, *108*, 6573−8.
(46) Klein, U.; Lia, M.; Crespo, M.; Siegel, R.; Shen, Q.; Mo, T.; Ambesi-Impiombato, A.; Califano, A.; Migliazza, A.; Bhagat, G.; Dalla-Favera, R. *Cancer Cell* **2010**, *17*, 28−40.
(47) Calin, G. A.; Liu, C. G.; Sevignani, C.; Ferracin, M.; Felli, N.; Dumitru, C. D.; Shimizu, M.; Cimmino, A.; Zupo, S.; Dono, M.; Dell'Aquila, M. L.; Alder, H.; Rassenti, L.; Kipps, T. J.; Bullrich, F.; Negrini, M.; Croce, C. M. *Proc. Natl. Acad. Sci. U. S. A.* **2004**, *101*, 11755−11760.
(48) Calin, G. A.; Ferracin, M.; Cimmino, A.; Di Leva, G.; Shimizu, M.; Wojcik, S. E.; Iorio, M. V.; Visone, R.; Sever, N. I.; Fabbri, M.; Iuliano, R.; Palumbo, T.; Pichiorri, F.; Roldo, C.; Garzon, R.; Sevignani, C.; Rassenti, L.; Alder, H.; Volinia, S.; Liu, C. G.; Kipps, T. J.; Negrini, M.; Croce, C. M. *N. Engl. J. Med.* **2005**, *353*, 1793−1801.
(49) Zhang, J.; Jima, D. D.; Jacobs, C.; Fischer, R.; Gottwein, E.; Huang, G.; Lugar, P. L.; Lagoo, A. S.; Rizzieri, D. A.; Friedman, D. R.; Weinberg, J. B.; Lipsky, P. E.; Dave, S. S. *Blood* **2009**, *113*, 4586−4594.
(50) Fulci, V.; Chiaretti, S.; Goldoni, M.; Azzalin, G.; Carucci, N.; Tavolaro, S.; Castellano, L.; Magrelli, A.; Citarella, F.; Messina, M.; Maggio, R.; Peragine, N.; Santangelo, S.; Mauro, F. R.; Landgraf, P.; Tuschl, T.; Weir, D. B.; Chien, M.; Russo, J. J.; Ju, J.; Sheridan, R.; Sander, C.; Zavolan, M.; Guarini, A.; Foa, R.; Macino, G. *Blood* **2007**, *109*, 4944−4951.
(51) Xiao, Y.; Lai, R. Y.; Plaxco, K. W. *Nat. Protoc.* **2007**, *2*, 2875−2880.
(52) Gorodetsky, A. A.; Barton, J. K. *Langmuir* **2006**, *22*, 7917−7922.
(53) Boon, E. M.; Salas, J. E.; Barton, J. K. *Nat. Biotechnol.* **2002**, *20*, 282−286.
(54) Boon, E. M.; Barton, J. K.; Pradeepkumar, P. I.; Isaksson, J.; Petit, C.; Chattopadhyaya, J. *Angew. Chem., Int. Ed. Engl.* **2002**, *41*, 3402−3405.
(55) Gorodetsky, A. A.; Hammond, W. J.; Hill, M. G.; Slowinski, K.; Barton, J. K. *Langmuir* **2008**, *24*, 14282−14288.
(56) Boon, E. M.; Livingston, A. L.; Chmiel, N. H.; David, S. S.; Barton, J. K. *Proc. Natl. Acad. Sci. U. S. A.* **2003**, *100*, 12543−12547.
(57) Liu, H. H.; Lu, J. L.; Zhang, M.; Pang, D. W. *Anal. Sci.* **2002**, *18*, 1339−1844.
(58) Pheeney, C. G.; Guerra, L. F.; Barton, J. K. *Proc. Natl. Acad. Sci. U. S. A.* **2012**, *109*, 11528−11533.

DOI: 10.1021/ac504331c
Anal. Chem. 2015, 87, 1395−1403